Molecular Crystals and Liquid Crystals
Publication details, including instructions for authors and subscription information:
http://www.tandfonline.com/loi/gmcl16

Temperature Dependence and Anisotropy of Electron Drift Mobilities in Anthraquinone

Z. Burshtein [a] & D. F. Williams [a]

[a] Division of Chemistry, National Research Council of Canada, Ottawa, Ontario, Canada, K1A OR6

Version of record first published: 28 Mar 2007.

To cite this article: Z. Burshtein & D. F. Williams (1977): Temperature Dependence and Anisotropy of Electron Drift Mobilities in Anthraquinone, Molecular Crystals and Liquid Crystals, 43:1-2, 1-11

To link to this article: http://dx.doi.org/10.1080/00268947708084930

Mol. Cryst. Liq. Cryst., 1977, Vol. 43, pp. 1–11

Printed in Holland

Temperature Dependence and Anisotropy of Electron Drift Mobilities in Anthraquinone†

Z. BURSHTEIN and D. F. WILLIAMS

Division of Chemistry, National Research Council of Canada, Ottawa, Ontario, Canada K1A 0R6

(*Received December 13, 1976*)

Electron drift mobilities have been measured in anthraquinone single crystals by the transient photoconductivity technique. At low temperatures the mobilities are trap controlled with trap depth of about 0.2 eV and concentration of about 100 p.p.m. At room temperature and above, the mobilities are practically trap free, 0.28, 0.20 and 0.022 cm^2/V sec for the c', b and a crystallographic directions, respectively.

Theoretical calculations do not predict the observed mobility anisotropy. Some possible reasons for this discrepancy, such as anisotropy of electron–phonon coupling, or underestimation of the role of the oxygen substituents in electron exchange are discussed.

I INTRODUCTION

An understanding of the conductance process in organic materials is increasing in importance, recognizing their potential in, for example, solar energy studies as either a photovoltaic material or a photovoltaic sensitizer. The existence of an enormous variety of organic compounds, commercially available and often quite cheap, enables us to introduce chemical changes into compounds which can affect electron exchange and/or electron phonon interactions and hence give insight into the details which determine charge carrier transport. Accordingly we have started to study a series of crystals with the same basic crystallographic structure as the archtype molecular crystal, anthracene.

The first successful experimental measurements of charge carrier mobilities in anthracene were made by Kepler.[1] His transient photoconductivity technique, by which the drift mobility of photogenerated charge carriers is determined from their transit time across the crystal is still the most useful.

Theoretical calculations of charge carrier mobilities soon followed the first experimental measurements. As is generally the case, these calculations have steadily become more complex, though the approach has remained reasonably constant. In the first step one calculates the charge carrier band structure, which is a straightforward though elaborate procedure.

To obtain mobility values from these bandwidth calculations requires an evaluation of the electron–phonon interactions for the crystal. Usually these interactions are introduced phenomenologically through an adjustable mean free time or mean free path. In spite of the obvious difficulties, such as the complexity of inter and intra molecular vibrations, the calculations for the simple aromatic hydrocarbon crystals such as anthracene showed the carrier bands were narrow and highly anisotropic, and quite well predicted the order of the mobility in the various crystal directions. Unfortunately such calculations on substituted aromatic crystals are sparse, and anthraquinone appears to be the only material for which band structures have been predicted. Naturally a comparison of measured mobilities with these calculations will help us to understand the role of substituents in the conductance process, for this reason anthraquinone was chosen as the first choice of material in a study of a series of crystals with the same crystallographic structure as anthracene, i.e. monoclinic with two molecules per unit cell.

II EXPERIMENTAL

The measurements were made on anthraquinone crystals grown from the melt by the Bridgman method. The starting material was purified by chromatography through an alumina column with benzene as a solvent. The purified material was heated to about 150°C under vacuum, and then sublimed into the growing tube. Unfortunately it is impossible to zone-refine anthraquinone effectively, as it tends to decompose at temperatures above the melting point (285°C). Indeed, while growing the crystal, some decomposition was observed, for the liquid phase slowly darkened in color. However, most of the decomposition products remained in the molten zone at the top of the growing tube, thus being removed from the growing crystal. The crystals showed no gradation in color. As will be shown in the following section, the samples grown contained an appreciable density of traps, however, they were apparently purer than crystals prepared by others[2] where electron transit-times could not be resolved. Samples, typically 5 mm × 5 mm × 1 mm, were cut by a wire saw and then polished on ethanol-soaked filter paper. Crystallographic alignment of the samples was performed by standard X-ray techniques.

A pulsed nitrogen laser which provided short light pulses (12–15 nsec) of wavelength[3] 3371 Å and integrated intensity of $\sim 10^{-3}$ J was used for the charge carrier generation. The sample was sandwiched between a transparent conducting glass which served as a front electrode, and a brass plate mounted on soft springs which acted as the back electrode. The crystal holder was mounted in a liquid nitrogen dewar. The temperature of the sample could be lowered below room temperature by increasing the amount of liquid nitrogen contained in the dewar, or increased above room temperature by flowing hot air. The temperature was monitored by a copper–constantan thermocouple. The high voltage across the sample was provided by a 410 Fluke High-Voltage power supply. Upon excitation with the laser pulse, as the current flowed into the crystal, a parallel voltage was developed over a series resistor. This voltage was fed into a source-follower F.E.T. whose output was displayed on an oscilloscope screen and photographed with polaroid film. Both the oscilloscope and the nitrogen laser were triggered with a 214A Hewlett Packard pulse-generator. Experiments made on anthracene crystals gave mobilities equal to literature values.

III RESULTS AND DISCUSSION

Figure 1 shows some typical current transients measured when the laser light was focused onto the crystal while the front electrode was negatively biased. When the illuminated (front) electrode was positive, no photocurrents related to holes could be detected. Therefore, in the present study we can report on electron mobility only. It is worthwhile to mention that hole photocurrents reported by Oyama and Nakada[2] were actually electron photocurrents originating at the counter electrode produced by the light which has penetrated through the crystal. By repeating their measurements

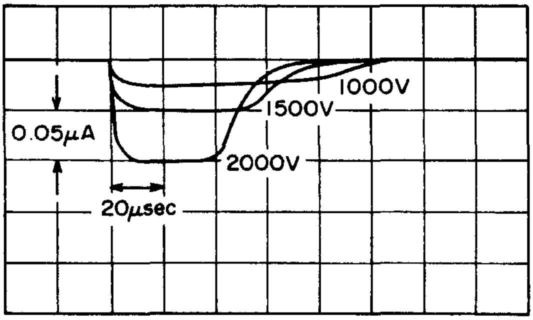

FIGURE 1 Typical room temperature electron transients for various voltages. Electric field in c' direction. Sample thickness 1.50 mm.

with crystals of various thicknesses, this point was unequivocally established. It thus appears that hole photogeneration is many orders of magnitude less efficient when compared to electron photogeneration in anthraquinone.

The particular current transients of Figure 1 were taken at room temperature with the electric field parallel to the crystal c' direction. The photocurrent transients revealed all the characteristics expected if the charge carrier generation took place in a narrow region close to the sample's surface, and the generation time was short compared to the charge carrier transit time across the sample. The width of the generation region is 1 μm at most in view of the high absorption coefficient of the crystal at the wavelength of excitation.[4] For these conditions, the electron transit time t_t is given by[1]

$$t_t = \frac{L^2}{\mu V}, \tag{1}$$

where L is the sample's thickness, V the voltage between the electrodes and μ is the electron mobility. The transit time for each trace in Figure 1 is determined from the kink by which the current ends. Eq. (1) predicts the transit time is inversely proportional to the applied voltage, and this relationship was observed as can be seen in Figure 2. The experimental points fall on a straight line intersecting the origin, as expected (Eq. (1)). Similarly the L^2 dependence of t_t was also confirmed. The room temperature electron mobilities were determined to be 0.28 cm^2/V · sec, 0.20 cm^2/V · sec and 0.022 cm^2/V · sec for the c', b and a crystallographic directions respectively.

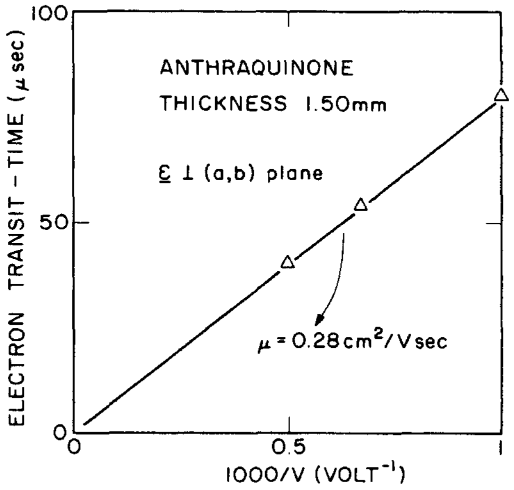

FIGURE 2 The transit time t_t as a function of 1000/V. Data taken from Figure 1.

It should be mentioned that no space charge effects were observed, though in some cases (for thinner crystals) the current density through the illuminated region (3–5 mm^2) was quite high. The parallel capacitance of the rest of the electrodes area (~ 1 cm^2) together with that due to the electrical leads was measured to be about 10–12 pF, and it is this which is responsible for the suppression of space charge effects.

The electron mobility was studied in detail as a function of temperature for the various crystallographic directions, and the results are represented in Figure 3. Here, the electron mobility is plotted versus $1000/T$, where T is the absolute temperature, on a semi-log scale. The principal mobility tensor directions are found to be the a, b and c' ($\perp$ to (a, b) plane) crystallographic directions.[5] The mobilities in these directions are shown in the figure. The largest mobility was measured for the c' direction, and the smallest, about 10 times smaller, for the a direction. In all directions the electron mobilities

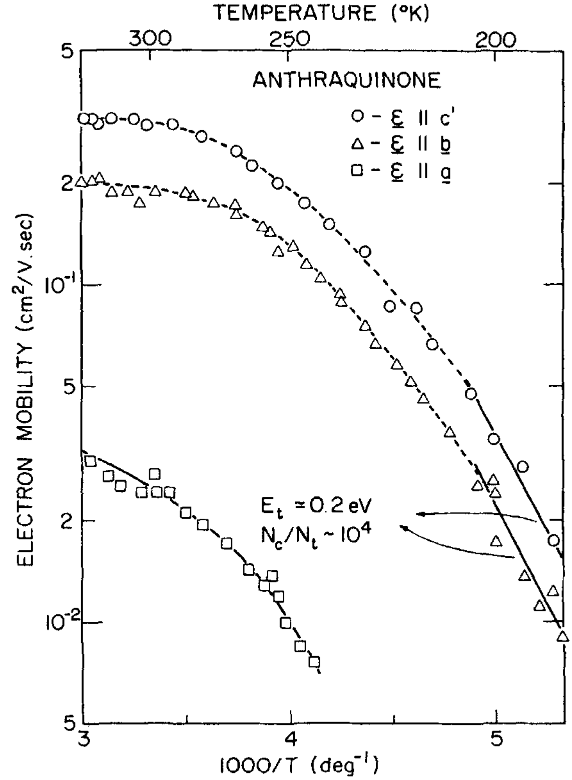

FIGURE 3 Semi-log plot of electron mobility vs. $1000/T$ for the principal mobility tensor axes.

decrease with decreasing temperature for temperatures below ~250°K, and saturate at about room temperature (~300°K). The low temperature mobilities can be described as a thermally activated mobility, with an activation energy E_t of about 0.2 eV for both b and c' direction. It appears to be the same also for the a direction, though the lack of data in the lower temperature region prevented us from satisfactorily calculating the activation energy.

A behavior such as described above is typical of a case where the low temperature mobility is controlled by multiple events of trapping and detrapping during a transit of the charge carrier across the crystal[6] (trap controlled mobility). Since the charge carrier spends some time being immobile, its effective mobility μ^* calculated from the measured transit time is reduced according to

$$\mu^* = \mu_0\left[1 + \left(\frac{N_t}{N_c}\right)\exp\left(\frac{E_t}{k_B T}\right)\right]^{-1}, \tag{2}$$

where μ_0 is the lattice (trap-free) mobility, N_c is the conduction band effective density of states, N_t is the trap density and E_t its depth below the conduction band edge. This formula is correct on condition that both the trapping-time and the release time are short compared to the transit time. Also, it is valid in the above form only for the limiting case where the motion of the excess electron can be described within the frame of the band model approximation. It can be generalized to the case when the lattice mobility falls within the frame of the small polaron hopping model by multiplying the pre-exponential term in Eq. (2) by an attempt-to-escape frequency ratio term.[7]

If we assume that for our case the attempt-to-escape frequency ratio is of the order of unity the ratio N_c/N_t is estimated to be about $\sim 10^4$. This assumption will be justified later on. An upper limit estimate for N_c is given by the density of anthraquinone molecules. The content of "impurities," chemical and physical defects, which give rise to the carrier trapping effect is less than about 100 p.p.m. Their main origin is likely to be the decomposition which takes place at the high temperature needed for growing the crystal from the melt.

In the frame of the model for trap-controlled mobility, the values of the mobility measured above room temperature describe the true lattice mobility. In this temperature range, the thermal de-trapping process is so fast that the traps play no role in determining the drift velocity. Though the available temperature range is quite narrow, one can still conclude that in that range there is little, if any, change of mobility with temperature. This holds for all crystallographic directions.

A central problem of charge carrier transport in organic solids is whether the proper description is by the band model[8] or by the small polaron hopping model.[9] In the band model the charge carrier is described by a Bloch-type wave function. The thermal vibrations are considered to be a small perturbation which scatters the charge carrier between the different Bloch states. Increasing the temperature increases the phonon population, hence the rate of scattering. The mobility will therefore decrease. For the small polaron hopping model the situation is different. The excess electron is localized on one molecule for a sufficient length of time to polarize its vicinity and hence reduce its energy. The carrier then is trapped (self-trapping). The thermal vibrations may occasionally bring the electronic energy levels of the occupied site into momentary coincidence with an empty state on a neighboring site. In this situation it is very likely that the charge carrier will tunnel, or hop to the new site. This is a thermally activated process; the higher the temperature the higher the hopping rate, hence the mobility. In the intermediate case between the two models one would expect to observe no temperature dependence. A detailed theory for this intermediate case is still lacking. It is estimated,[10] on the basis of the uncertainty principle, that for molecular crystals the band model would be consistent with mobilities larger than the order of ~ 1 cm^2/V · sec at room temperature, while the small polaron hopping model[11] would be consistent with mobilities smaller than about ~ 0.1 cm^2/V · sec.

The experimental room temperature lattice mobilities of anthraquinone obtained in the present work are in the range expected to be in the intermediate region between the two models. The lack of significant temperature dependence is thus well expected. Also it justifies the approximation previously mentioned that the attempt-to-escape frequency ratio should be of the order of unity.

There is yet another possible way to account for the temperature dependence of the mobility that should be considered. Within the hopping model itself at high temperatures there should be a transition from a thermal activation to a $T^{-3/2}$ dependence of the mobility on temperature.[9] This happens when the thermal energy $k_B T$ is large enough that it is comparable to half of the polaron binding energy W_p. The observed temperature saturation of the mobility could be interpreted as that transition. However, in that case the activation energy at low temperatures, 0.2 eV, should equal $(\frac{1}{2})W_p$. The measured temperature where saturation actually occurs is thus much too low to account for the measured activation energy for mobilities at low temperatures. Thus this model does not apply to anthraquinone.

Quite recently, calculations of the charge–carrier transport in anthraquinone have been performed[12] following the same general method used for anthracene, but taking into account the electronegativity of the oxygen compared to carbon atoms. The electron bandwidths were found to be highly anisotropic, namely 0.02 eV, 0.35 eV and 0.013 eV in the a, b and c'

crystallographic directions, respectively. Though for aromatic hydrocarbons band structure calculations do predict reasonably well the ordering of the mobilities in the crystallographic directions, this is obviously not so for anthraquinone, in which the mobilities are 0.022, 0.20 and 0.28 $cm^2/V \cdot sec$ in the *a*, *b* and *c*′ directions respectively.

It is worthwhile at this stage to visualize the crystal structure of anthraquinone.[5] In Figure 4(a) are shown the unit cell dimensions, while Figure 4(b) shows the locations of seven molecules projected along the *c*′ direction. The centers of all the molecules shown in the figure are in the (*a*, *b*) plane. The

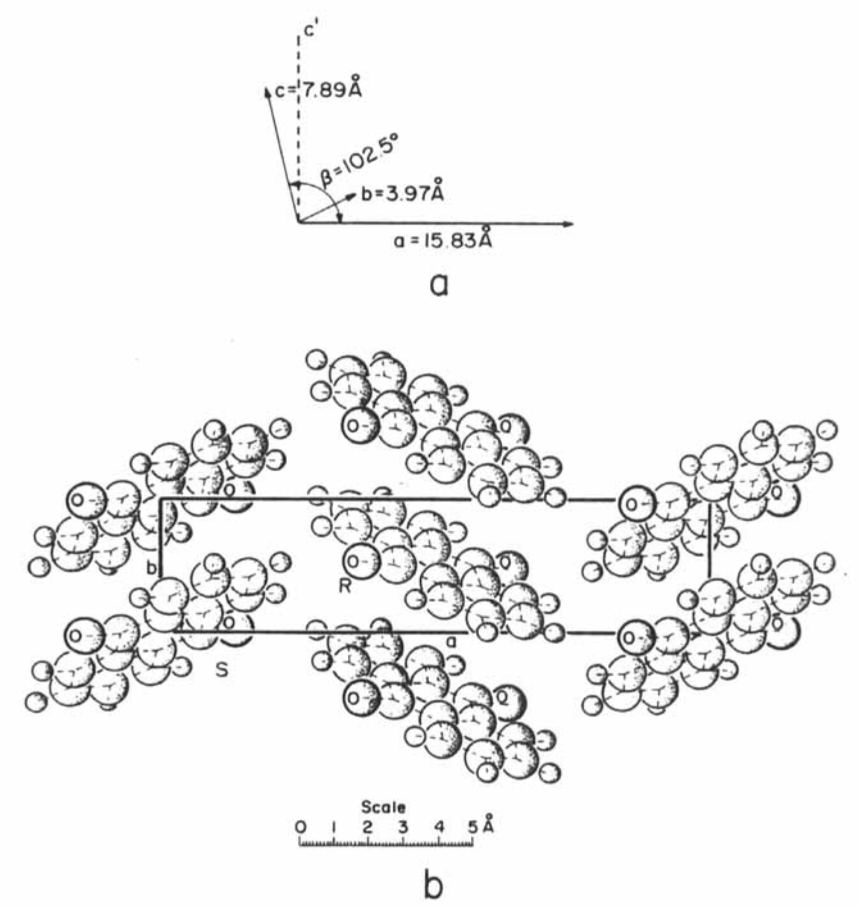

FIGURE 4 The crystal structure of anthraquinone: (a) unit-cell dimensions, (b) projection of molecular arrangement along the *c*′ direction. The small size circles indicate the hydrogen atoms. The letters *S* and *R* denote the standard and reflected molecules, respectively, which together constitute the pair of molecules attached to each lattice point to form the crystal.

crystal is made up from such layers mounted one on top of another along the *c* direction. Along the *b* direction the electronic overlap is mainly through the molecular planes and is therefore the biggest. In the *a* and *c′* directions the electronic wave-functions overlap only through the sides of the molecules, hence the narrowness of the bands in those directions.

In order to properly predict the actual values of the mobility in the various directions from the respective bandwidths it is essential to know the scattering rate, or to make reasonable assumptions concerning carrier scattering: either a constant mean free path λ_0 or a constant mean scattering time τ_0 for the charge carrier. The assumption of a constant mean scattering time τ_0 predicts the largest mobility in the *b* direction, and much smaller mobilities in the *a* and *c′* directions.[12] Upon accepting these electron exchange calculations one must conclude that the scattering process is very anisotropic. To estimate the ratio of the mean scattering times at the various directions a knowledge of the electron velocity components is necessary. As already mentioned the band model is not really a good theoretical description of electronic transport in anthraquinone, but it should still give a rough approximation of the values of the velocity components. Using the values computed by Mathur and Kumar[12] one obtains the ratios $\tau_{aa}/\tau_{bb} \sim 10$, and $\tau_{c'c'}/\tau_{bb} \sim 100$, where τ_{aa}, τ_{bb} and $\tau_{c'c'}$ are the mean scattering times for electrons along the *a*, *b* and *c′* directions, respectively. It has already been pointed out by Kubarev and Michailov[13,14] that the scattering time components should depend on the bandwidth, being shorter for wider bands. The reason is that for wider bands more phonon frequencies are able to scatter the charge carrier between states within the band. In particular, for the *b* direction of anthraquinone, where the bandwidth has been estimated as 0.35 eV, many of the molecular vibrational modes can participate in the scattering process. Indeed, the possibility that the scattering time for a certain direction could be inversely proportional to the charge carrier bandwidth in that direction was presented in the mobility calculations of Mathur and Kumar.[12] Unfortunately, however, the model still fails to predict the measured mobility anisotropy. It seems, therefore, that more elaborate work on the scattering of charge carriers is substituted organic crystals is needed before theoretical calculations are able to predict even the anisotropy of the mobility tensor.

However it should be remembered that we have assumed the band structure calculations are satisfactory. The good agreement between such calculations and experimental results for the simple aromatic hydrocarbons is well known. Perhaps anthraquinone illustrates a further important point which should be considered. A careful examination of the crystallographic structure of anthraquinone[5] reveals that the shortest distance between an oxygen atom on one molecule and a ring carbon atom on the neighboring molecule which is displaced along the *c* direction is only 3.52 Å. This is even shorter than the intermolecular gap along the *b* direction [see Figure 4]. Thus our experimental results could be rationalized without the need for an anisotropic relaxation time provided the sp^2 hybrid orbitals of the oxygen of the neutral molecule can participate in the conductance process, i.e. these orbitals can mix to some extent with the π orbitals when the excess electron is introduced. It should be noted that since the mobilities are all low, very little overlap in this direction would be sufficient to give rise to the observed mobilities. For aromatic hydrocarbons this situation does not arise, and only π orbitals are important, and naturally only the π orbitals were considered by Mathur and Kumar[12] in their band structure calculations. Some support for a slight mixing of these oxygen orbitals can be seen when we consider the difference in bond order for the C=O bond in a neutral molecule and in the anion. With simple Hückel theory, it is seen that this bond order is reduced from ~1.71 to ~1.56.[15] This is a considerable decrease, and could weaken the double bond character enough to give sufficient mixing of the sp^2 oxygen orbitals with the molecular π orbitals to account for the observed mobilities. Obviously the effects of this bond order decrease cannot be quantized at present. but it certainly appears to be significant. This is shown when we compare the properties of stilbene, $\phi{-}C{=}C{-}\phi$, in the neutral and anion forms. The neutral molecule exists in two stable forms, cis and trans, and a considerable energy ~2.0 eV is required[16] to change either form to the other, via a rotation of the ϕ (phenyl) groups around the central C=C bond. The anion of stilbene however has only been observed in the trans configuration, no matter if cis or trans stilbene is the starting material, which means rotation around this C=C bond is relatively easy in the anion. A similar reduction in bond order has occurred in the C=C bond in stilbene as occurred in the C=O bond in anthraquinone.

Band structure calculations in the spirit of these considerations together with experimental studies of mobilities for other substituted aromatics are in progress. It is hoped that these further results will aid in finding the role of substituents in carrier transport in aromatic hydrocarbons.

CONCLUSIONS

The electron drift mobilities in anthraquinone were measured using the transient photoconductivity technique. At low temperatures the mobilities are trap-controlled with trap depth of about 0.2 eV and concentration of about 100 p.p.m. At room temperature and above, the mobilities are practically trap-free, 0.28, 0.20 and 0.022 $\mathrm{cm^2/V \cdot sec}$ for the c', b and a crystallographic directions, respectively.

There exist two ways to account for the mobility anisotropy measured in the present work. If the band structure calculations by Mathur and Kumar[12] are correct, then the scattering time of the electron needs to be highly anisotropic. On the other hand it is suggested that the electron scattering is isotropic. In that case the large mobility in the c' direction can be explained by the involvement of the in-plane sp^2 hybridized orbitals of the oxygen atoms in the conduction process. Additional experimental evidence on other substituted hydrocarbons, as well as more theoretical work is necessary to clarify this interesting point.

Acknowledgement

We are indebted to Dr. A. W. Hanson for the crystallographic alignment of our samples.

References

† Issued as NRCC No. 16048.
1. R. G. Kepler, *Phys. Rev.*, **119**, 1226 (1960).
2. K. Oyama and I. Nakada, *J. Phys. Soc. Jap.*, **24**, 798 (1968).
3. D. Leonard, *Appl. Phys. Lett.*, **7**, 4 (1965).
4. J. W. Sidman, *J. Am. Chem. Soc.*, **78**, 4567 (1957).
5. K. Lonsdale, H. J. Milledge, and K. El-Sayed, *Acta. Cryst.*, **20**, 1 (1966).
6. D. C. Hoesterey and G. M. Leston, *J. Phys. Chem. Solids*, **24**, 1609 (1963).
7. D. C. Hoesterey and G. M. Leston, *J. Chem. Phys.* **41**, 675 (1964).
8. R. W. Munn and W. Siebrand, *J. Chem. Phys.*, **52**, 6391 (1970).
9. W. E. Spear, *Adv. Phys.*, **23**, 523 (1974).
10. S. H. Glarum, *Phys. Chem. Solids*, **24**, 1577 (1965).
11. H. Fröhlich and G. Sewel, *Proc. Phys. Soc.*, **74**, 643 (1959).
12. S. C. Mathur and B. Kumar, *Mol. Cryst. Liq. Cryst.* **23**, 85 (1973).
13. S. I. Kubarev and I. D. Mikhailov, *Theor. Exp. Chem.*, **3**, 265 (1967).
14. S. I. Kubarev and I. D. Mikhailov, *Theor. Exp. Chem.*, **4**, 134 (1968).
15. C. A. Coulson and A. Streitweiser, Jr., *Dictionary of π electron calculations* (W. H. Freeman & Co., 1965).
16. G. B. Kistiakowsky and W. R. Smith, *J. Amer. Chem. Soc.*, **56**, 638 (1934).
    A. V. Santoro, E. J. Barrett, and H. H. Hoyer, *J. Amer. Chem. Soc.*, **89**, 4545 (1967).